JOURNAL OF OPTOELECTRONICS AND ADVANCED MATERIALS Vol. 9, No. 5, May 2007, p. 1317 - 1321

Study of the structure and the corrosion performance of tin plasma sprayed coatings

G. VOURLIAS*, N. PISTOFIDIS, G. STERGIOUDIS, E. K. POLYCHRONIADIS
Physics Department, Aristotle University of Thessaloniki, 54 124 Thessaloniki, Greece

Tin (Sn) is characterized by excellent corrosion resistance in aqueous environments at low temperature. Therefore this metal is used as a coating for iron. The usual method for the tin deposition is hot-dipping. However, this method, although it is very effective, it is not environmentally friendly. Consequently, alternative methods are investigated, one of which is plasma spraying. In the present work strips of steel St-37 were coated with tin (Sn) with plasma spraying. Initially their structure was studied with scanning electron microscopy (SEM), X-ray diffraction (XRD) and conventional transmission electron microscopy (CTEM). From this research it was deduced that the coating is mainly composed of tetragonal tin with very low porosity, while a tin oxide film is likely to cover its surface. Finally CTEM showed that Fe-Sn phases are formed. Afterwards the coatings were exposed in a salt spray chamber (SSC). The as-corroded samples were studied with optical microscopy, SEM and XRD and it was concluded that Sn and Fe oxides and chlorides were formed on the coating surface along with large cavities. A possible mechanism of internal oxidation (intergranular corrosion) was used to explain these observations, while an effort was made to correlate the coating structure with the corrosion results.

(Received November 14, 2006; accepted April 12, 2007)

Keywords: Metals and alloys, Plasma spray, Tin, Coating materials, X-ray diffraction, SEM, TEM

1. Introduction

Tin (Sn) is one of the oldest known metals. It was used by many ancient civilizations because it forms bronze alloyed with copper - which gave its name to the Bronze Age [1]. In modern times tin is still widely used, although it is very soft and because of its low strength the pure metal is not regarded as a structural material. Rather, pure tin is most frequently used as coating for iron to impart corrosion resistance and enhance appearance [2].

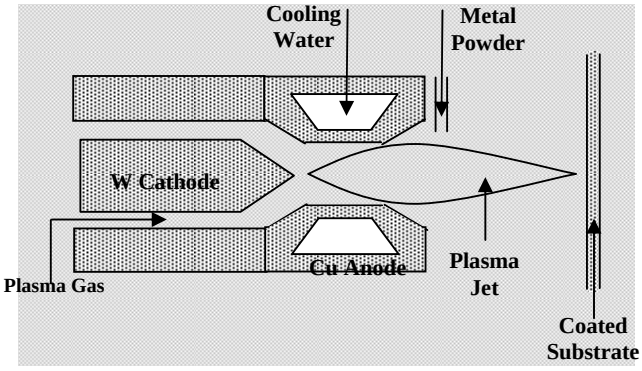

Fig. 1. Schematic drawing of a plasma spraying device (plasma gun).

In the case of ferrous substrates tin coatings are mainly used in the food packaging (tinplate) since, apart from the fact that they offer excellent corrosion protection from fatty acids and biological fluids [2-3], they are inexpensive and not hazardous to human health [4]. However it is also used for heavier coatings applied to individual components by batch processing for non-packging applications, such as food-processing equipment, electrical and electronic components, wires and fasteners. The usual method for the tin deposition is hot-dipping [2-3]. Nevertheless, this method, even though it is very effective, it is not environmentally friendly, because it is characterized by a large volume of harmful byproducts [3]. Consequently, alternative methods are investigated which could be used instead of hot-dipping. A well-promising technique is plasma spraying [5-6]. A simplified diagram of a plasma spray device is shown in Fig. 1. An electric arc of high intensity (a few hundred amperes) between a tungsten cathode and a copper anode ionizes the plasma gas (e.g. Ar) forming the plasma jet. The metallic powder is fed at the exit point of the jet from the aperture of the device, where it melts. The droplets, accelerated by the plasma gas, strike the surface of the substrate, flatten and form thin lamellae that conform, adhere and interlock with each other and the substrate surface building up a metallic layer up to a thickness of a few hundreds of μm [7-9].

The structure and the morphology of tin plasma sprayed coatings have been reported elsewhere [10-12]. In this work the corrosion performance of these coatings is examined, because, although the corrosion of tin is a well-studied phenomenon [2], the corrosion behaviour of plasma sprayed coatings is not studied in details [13]. In this project the corrosion phenomena were accelerated in a salt spray chamber (SSC) and the investigation of the collected data was focused on the determination of the corrosion mechanism. For that purpose a brief overview of the coating structure is also presented. Since the information gathered is due only to the samples exposed in the SSC, no field data is available. As a result no modelling of the corrosion progress took place and only a qualitative study of the phenomenon was accomplished.

2. Experimental

Plates of steel St-37 of 15x3x0.3 cm^3 dimensions were used as substrates and were coated according to the following steps: (1) chemical cleaning with organic solvents, (2) grit blasting with Al_2O_3 particles in order to create an anchor tooth profile at the surface of the substrate (3) deposition of Sn. The plasma gas was an Ar mixed with He in order to increase its thermal conductivity and viscosity. The current intensity for the plasma formation was 650 Amperes and the deposited material was commercially available grade Sn in the form of gas-atomized powder with an average diameter of 110±10 μm as it was determined microscopically.

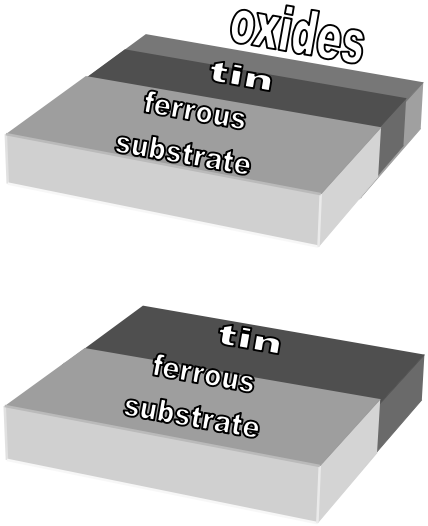

Fig. 2. Schematic representation of the sample preparation for the examination with XRD at different depths.

After the coating deposition, cross-sections of the as-sprayed specimens have been cut, mounted in bakelite and polished up to 5μm alumina emulsion for morphological observation. Their characterization took place with Scanning Electron Microscopy (SEM), X-Ray Diffraction (XRD) and Conventional Transmission Electron Microscopy (CTEM). SEM observations were performed with a 20kV JEOL 840A SEM equipped with an OXFORD ISIS 300 EDS analyzer and the necessary software. Stoichiometric microanalysis and chemical mapping was performed on the polished cross-sections of the coating. XRD took place with a Siemens D-8000 diffractometer with Bragg-Brentano geometry using CuKα radiation (λ=1.54186Å). The samples were twice examined. During the first examination the initial coating surface was exposed in the X-Ray beam. Afterwards part of the coating (about 80-100 μm in depth) was abrasively removed (Fig. 2) and the samples were re-examined in order to exclude the effect of phases formed only at the coating surface and to determine the effect of phases present only at the Fe/Sn interface since the X-Ray beam of the diffractometer cannot penetrate a tin layer with about 200 μm thickness (which is the average coating thickness). Finally, selected specimens, after the suitable preparation, were examined with CTEM by using a 100 kV JEOL 100CX TEM in order to determine the microstructural characteristics of the tin coating, as well as the resulted phases near the coating/substrate interface.

For the corrosion study, the samples were hanged vertically with nylon fibers at about the center of the working volume of a Salt Spray Chamber (SSC) SC-450. Their uncoated edges were covered with bee wax, in order to be isolated from the environment so as to avoid ion penetration from these sides. The corrosive medium was a 5 wt. % solution of NaCl in de-ionized water in order to simulate a marine atmosphere free of pollutants. The temperature of the chamber was 40°C while the relative humidity remained stable at 100%. Specimens were retrieved from the chamber after 24, 96, 192 and 240 hrs (1 day, 4 days, 8 days and 10 days respectively). The corroded samples were initially photographed with a Zeiss M8 stereoscope at low magnification connected with a digital camera. Afterwards cross sections from each specimen have been cut and after the suitable preparation were observed with an Olympus BX60 light microscope connected with a digital camera CCD JVC TK-C1381 and a personal computer. The nature of the phases has been determined using the above-mentioned methods. From this data conclusions about the corrosion mechanism were drawn.

3. Results and discussion

3.1 Characterization before corrosion

The initial observation of the coating cross-section (Fig. 3) revealed that the coating is characterized by high integrity. Especially along the interface with the substrate neither pores nor inclusions are observed. Therefore good coating adhesion is expected, while there are no paths that could facilitate diffusion into the coating. Nevertheless, certain cavities were detected inside the coating, some of which are noted with arrows in Fig. 3 and which seem to be unavoidable if we take into account the deposition method [6, 9]. However, they do not communicate with each other and they obviously refer to a very small percentage of the total volume of the coating. Hence it is rather impossible to affect the corrosion performance of the coating.

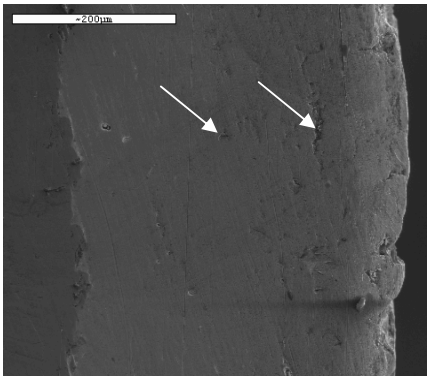

Fig. 3. SEM micrograph of the coating cross-section. The arrows indicate cavities in the coating.

EDS analysis revealed that the coating is composed, as it was expected, by almost pure Sn. Apart from tin,

oxygen is present up to about 20-30 μm from the surface resulting from the reaction of the tin surface with the atmospheric oxygen after the coating deposition. The presence of this layer inhibits further corrosion of the underlying tin and thus protects the coating [2]. Furthermore EDS analysis close at the Fe-Sn interface implies a certain diffusion of Fe in the coating, since Fe was detected over the Fe/Sn interface and the atomic radius of Fe is smaller than the atomic radius of Sn [18]. Concerning a coating of that kind, only low diffusion could be anticipated since the solidification of the coating is accomplished very quickly (within a few μsec, mostly depending on the thermal resistance at the interface [6]) and consequently only solid state diffusion takes place. In order to investigate this hypothesis the samples were examined with XRD (Fig. 4). The initial examination showed only the reflections of tetragonal tin and a few peaks of Sn oxides due to the initial exposure of the coating in the atmosphere. After the thickness reduction with abrasive removal, along with tin reflections, appeared also peaks referring to Fe, which originate from the substrate. This observation verifies that X-Rays penetrated up to the Fe/Sn interface. However it was not revealed any Fe-Sn phases probably due to the low concentration of these phases in the coating and to the low sensitivity of XRD. The limitations of XRD led to the examination of the Fe-Sn interface by Electron Diffraction (ED), which revealed polycrystalline areas composed by small or bigger crystallites of Fe-Sn phases (Fig. 5). The ED of Fig. 5a shows among others a large number of spots, which are located inside a circular area (denoted by "Δ" in Fig. 5a) belonging to several rings having slightly different radii. These rings belong to Fe-Sn phases having unit cell parameters slightly different by comparison to each other. This means that there is also a slight difference in their stoichiometry. In the case of Fig. 5b the recorded ED refers to a phase consisting by very fine crystallites which form complete rings in the ED. In this case the rings were indexed and it was verified that they refer to the Fe_3Sn_2 phase [14]. However, the rings are also broad, which means again that the stoichiometry of every crystallite is not exactly the same. In any case, the detection of Fe/Sn phases at the interface verified that diffusion takes place between the two phases. This phenomenon is very important because it ensures good contact of the coating to the substrate and hence good coating adhesion which renders the coating failure is less probable. As a result the corrosion protection is enhanced.

3.2 Corrosion performance

From the above examination three main conclusions could be drawn. First of all the coating is very compact. Thus there are no paths facilitating corrosion. Furthermore, the coating is very homogeneous from a compositional point of view. Hence there are no inclusions that could act as corrosion nuclei. Nevertheless, there is also a tin oxide layer that also protects the substrate. Finally, the fact that diffusion takes place at the Fe/Sn interface verifies that the coating adhesion is very good. As a result delamination is rather improbable and corrosion due to substrate stripping is not possible.

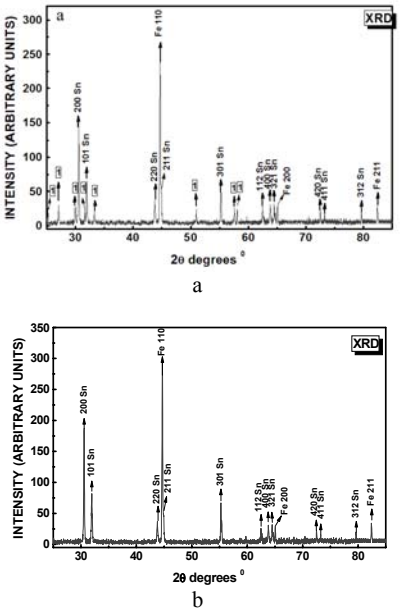

Fig. 4. XRD pattern of the Sn coating (a: without abrasive removal, b: after abrasive removal). The peaks noted with (1) refer to Sn oxides, while the rest of the peaks refer to tetragonal Sn (PDF#04-0673).

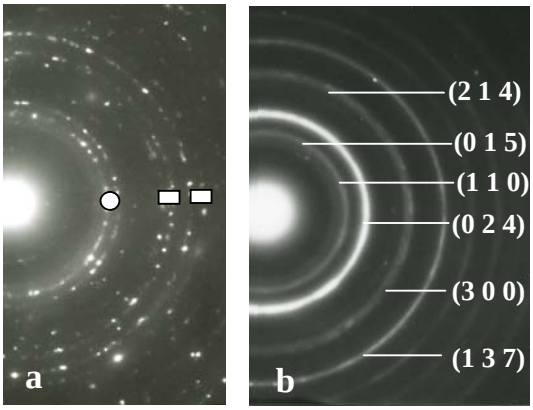

Fig. 5. ED patterns of the interface between the coating and the substrate (a: ED of Fe-Sn crystals of large size. The rings noted with "o" in Fig. 5a refer to several different Fe-Sn phases, while the rings noted with "Y" refer to Sn oxides. b: ED of small sized Fe_3Sn_2 crystals – PDF Card #71-0016 [14]).

Table 1. Experimental and calculated d-values for the indexed rings of the electron diffraction pattern of Fig. 5b.

hkl	d_{exp} (Å)	d_{cal} (Å)
015	3.00	3.01
110	2.68	2.672
024	2.10	2.097
214	1.65	1.649
300	1.55	1.542
137	1.17	1.669

The above statements imply that the coating exhibits very good corrosion resistance. However no conclusion could be drawn if the coatings are not examined after their exposure in a corrosive environment. For that purpose the coated samples were placed in a SSC and were examined after certain exposure periods which were previously mentioned. Some stereoscopic photographs at low magnification of the Sn samples after being retrieved from the SSC are presented in Fig. 6. The corrosion of the specimens is clearly observed. Their degradation began from the first day of exposure (Fig. 6a). The EDS analysis of the surface of the sample retrieved after 24 hrs (Fig. 6a) showed that tin (Sn), oxygen (O) and chlorine (Cl) along with iron (Fe) at different concentrations with regard to the examined point composed the corrosion products. Probably, even though only one day of exposure passed, tin chlorides had been already formed, if we take into account that tin oxides were already present. Also, the presence of iron (red rust) implies corrosion of the ferrous substrate. This phenomenon could not be ascribed to the iron content of the coating, since its content is very low and it is localized close at the Fe/Sn interface. Nevertheless, if we take into account that corrosion is a phenomenon highly affected by the specific properties and the inhomogeneities of every surface, in some areas, where the coating is thinner, its total failure is probable to lead to the substrate corrosion. Thus the formation of Fe oxides directly from steel is not impossible. In any case, since Sn is cathodic to iron and steel [15], the exposure of the substrate in an aqueous environment accelerates its corrosion. As a result, in accordance with the photographs of Fig. 6, the formation of these products expands uninterruptedly as long as the sample remains in the SSC.

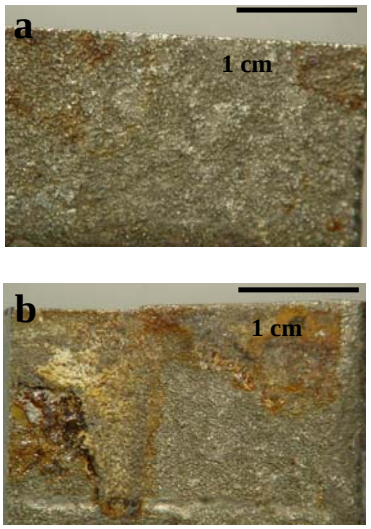

Fig. 6. Stereoscopic photos of the Sn coatings (a: after 24 hrs, b: after 10 days).

The determination of the composition of the corrosion products was accomplished with XRD (Fig. 7). This examination verified the formation of hydrated Sn oxides and chlorides along with similar Fe compounds. The comparison of the XRD shows also a progressive increase at the quantity of the compounds formed, as the intensity of the recorded peaks show. Consequently, as it was deduced from the stereoscopic photographs the formation of the corrosion products is continuing as long as the coating is in the SSC. Nevertheless more information could be collected from SEM micrographs (Fig. 8) of the cross section of the corroded coatings.

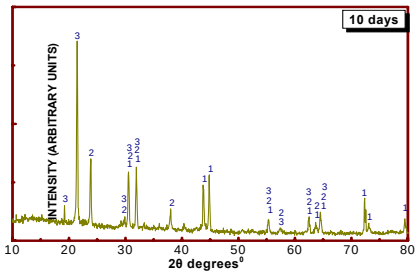

Fig. 7. XRD pattern of the corroded specimens (a: after 10 days). The peaks noted with (1) refer to pure Sn (PDF card#04-0673 [14]), the peaks noted with (2) to Sn hydrated chlorides (PDF cards#84-0929 and 76-1974 [14]) and the peaks noted with (3) to Sn oxides (PDF cards#78-1063 and 77-2296 [14]).

First of all the progressive character of corrosion is verified. As we see in Fig. 8a after 24 hrs in SSC the attack of the coating is very low. However as the exposure time increases, the corrosion becomes more severe. Cavities are formed, the depth of which is constantly increased and almost reaches the steel substrate. The chemical mapping of the cross-section is very enlightening concerning this phenomenon (Fig. 9). As Fig. 9 shows, the ions of O^{2-} and Cl^{-} are diffused in the coating, while they are present in the Sn-Fe interface at high concentration. This phenomenon is also verified with line scanning (Fig. 10). Consequently a mechanism of internal oxidation (intergranular) could be proposed. In this case the corrosive ionic species (oxygen and chlorine) diffuse in the coating especially along the grain boundaries [16-17]. As a result soluble Zn compounds are formed and entire grains are detached from the coating because their boundaries are decomposed with comparatively little corrosion of the grains. Furthermore the steady decrease of the coating shows that apart from internal oxidation the coating is also prone to uniform corrosion.

4. Conclusions

From the above investigation it turned out that:

- The main products of the aqueous corrosion of Sn coatings casted with plasma spraying are Sn and Fe chlorides and oxides.
- The decomposition of these coatings probably proceeds through a mechanism of internal oxidation which occurs with the diffusion of O^{2-} and Cl^{-} in the coating, while uniform corrosion is also observed. In general, although the mass loss is rather fast the protection is not inferior. Similar results were recorded for zinc which is the main competitive material [16-17]. Hence tin could be used instead in cases like the food processing equipment where zinc is not accepted.

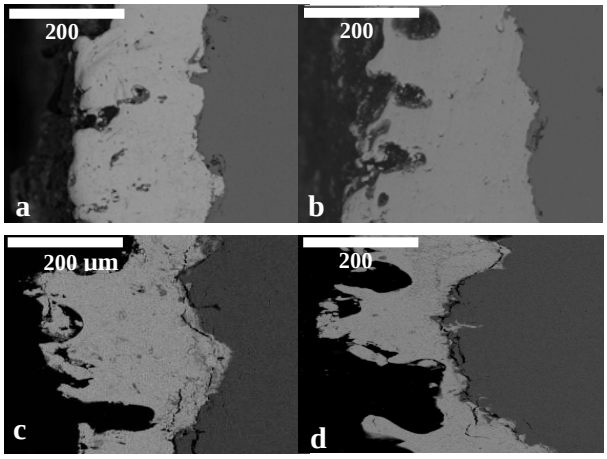

Fig. 8. SEM micrographs of the cross section of the corroded coatings (a: after 24 hrs, b: after 4 days, c: after 8 days, d: after 10 days).

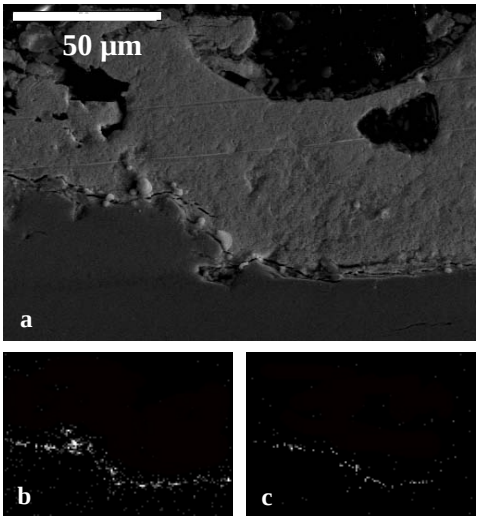

Fig. 9. Chemical mapping of the cross-section of the corroded coatings after 10 days of exposure in the SSC (a: SE micrograph, b: oxygen distribution, c: chlorine distribution).

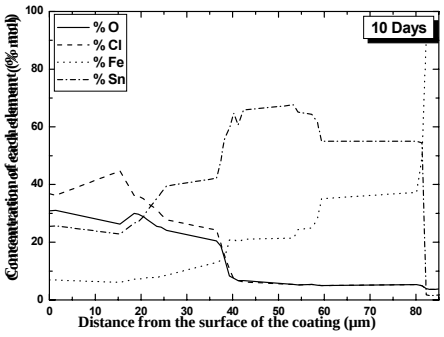

Fig. 10. Line scan of the corroded samples after 10 days of exposure in the SSC..

References

[1] D. A. Scott: Metallography and Microstructure of Ancient and Historic Metals, The J. Paul Getty Museum, Singapore (1991).
[2] ASM Handbook, Vol. 13-Corrosion, ASM, New York (1999).
[3] D. R. Gabe, Principles of Metal Surface Treatment and Protection, Pergamon Press, London (1978).
[4] N. Irving-Sax, Dangerous Properties of Industrial Materials, VNR, New York (1979).
[5] H. Herman, S. Sampath, R. McCune, Mat. Bull. **25**, 17(2000).
[6] ASM Handbook, Vol. 13-Corrosion, ASM, New York, (1999).
[7] S. Amada, K. Tomayasu, M. Haruyama, Surf. Coat. Tech. **96,** 176(1997).
[8] R. Ghafouri-Azar, S. Shakeri, S. Chandra, J. Mostaghimi, Int. J. Heat Mass Trans. **46**, 1395 (2003).
[9] Y. Chen, G. Wang, H. Zhang, Th. Sol. Fil. **390**, 13(2001).
[10] N. Pistofidis, G. Vourlias, E. Pavlidou, P. Patsalas, G. Stergioudis, E. K. Polychroniadis, D. Tsipas, Surf. Coat. Tech., in press, doi:10.1016/j.surfcoat.2005.11.085 (2006).
[11] G. Vourlias, N. Pistofidis, P. Patsalas, E. Pavlidou, G. Stergioudis, E.K. Polychroniadis, High Temp. Mat. Proc. **9**, 243(2005).
[12] G. Vourlias, N. Pistofidis, G. Stergioudis and E.K. Polychroniadis, J. All. Comp. in press, doi:10.1016/j.jallcom.2005.09.007 (2006).
[13] G. Vourlias, N. Pistofidis, D. Chaliampalias, E. Pavlidou, G. Stergioudis, E. K. Polychroniadis, D. Tsipas, Surf. Inter. Anal. **38**, 255(2006).
[14] PC Powder Diffraction Files for Windows, Version 2.02, JCPDS-The International Centre for Diffraction Data, (2000).
[15] M.G. Fontana, Corrosion Engineering, McGraw-Hill, New York (1986).
[16] G. Vourlias, N. Pistofidis, G. Stergioudis, D. Tsipas, Crys. Res. Tech. **39**, 23(2004).
[17] G. Vourlias, N. Pistofidis, G. Stergioudis, E. Pavlidou, D. Tsipas, Phys. Stat. Sol. A **201,** 1518(2004).
[18] D.R. Lide (Ed.), CRC Handbook of Chemistry and Physics, 80th ed., CRC Press, London (1999–2000).

*Corresponding author: gvourlia@auth.gr

JOURNAL OF OPTOELECTRONICS AND ADVANCED MATERIALS Vol. 9, No. 5, May 2007, p. 1317 - 1321